ЖЭТФ, 2012, том 142, вып. 1 (7), стр. 104–114

ANNIHILATION OF $\bar{p}+p \to e^+ + e^- + \pi^0$ AND $\bar{p}+p \to \gamma + \pi^0$ THROUGH AN ω-MESON INTERMEDIATE STATE

E. A. Kuraev [a*], ***Yu. M. Bystritskiy*** [a**], ***V. V. Bytev*** [a***], ***A. Dbeyssi*** [b****], ***E. Tomasi-Gustafsson*** [b†]

[a] *Joint Institute for Nuclear Research*
141980, Dubna, Moscow Region, Russia

[b] *Université Paris-Sud, Institut de Physique Nucléaire*
91405, Orsay, France

Received October 23, 2011

The s-channel annihilation of a proton and an antiproton into a neutral pion and a real or virtual photon followed by lepton pair emission is studied. Such a mechanism is expected to play a role at moderate values of the total energy $\sqrt{s}$, when the pion is emitted in the angular region around 90° in the center-of-mass system. A fair comparison with the existing data is obtained taking scattering and annihilation channels into account. The cross section is calculated and numerical results are given in the kinematical range accessible in the PANDA experiment at FAIR.

1. INTRODUCTION

The antiproton–proton annihilation in various leptonic and hadronic channels will be intensively studied by the PANDA collaboration [1] at the complex accelerator FAIR (Darmstadt), where it is planned to accelerate antiproton beams with the momentum from 1.5 to 15 GeV/c and average luminosity $\mathcal{L} = 1.6 \cdot 10^{32}\ \mathrm{cm}^{-2} \cdot \mathrm{s}^{-1}$ [2]. The $\bar{p}p$ annihilation into leptonic channels is very challenging because the hadronic background is higher by orders of magnitude. In Refs. [3, 4], the annihilation reaction $\bar{p}+p \to \gamma^* \to e^+ + e^-$ was investigated with the aim to extract of electromagnetic form factors of the proton in the time-like region. In this paper, we focus on the annihilation reactions

$$\bar{p}+p \to \gamma^* + \pi^0 \to e^+ + e^- + \pi^0, \tag{1}$$

$$\bar{p}+p \to \gamma + \pi^0, \tag{2}$$

which also contain interesting information, from different standpoints. Through the emission of one virtual photon between the proton–antiproton and the lepton pair, reaction (1) constitutes a unique opportunity to determine time-like proton form factors in the "unphysical" kinematical region, i. e., below the threshold of $\bar{p}+p$ annihilation into a lepton pair (i. e., for $0 < q^2 < 4M_p^2$, where q^2 is the momentum transferred to the proton and M_p is the proton mass) [5]. Related processes are the pion electroproduction on the proton, $e^- + N \to e^- + N + \pi$, which is under intensive experimental and theoretical study [6], and the pion-induced lepton pair production $\pi + N \to N + \ell^- + \ell^+$, first investigated in [7]. Pion scattering on nucleons and nuclei is part of the experimental program of the HADES collaboration [8]. Reaction (1) was studied in Ref. [9] near the threshold. In Ref. [5], the calculation was extended by introducing a larger set of diagrams and studying the sensitivity to different parameterizations of proton form factors. It was also suggested to extract information of the time-like nucleon axial form factor from the production of a charged pion in the reaction $\bar{p}+n \to e^+ + e^- + \pi^-$. Because no data exist for the nucleon axial form factor in the time-like region, predictions have been built on analytic extension of models that reproduce the data in the space-like region [10].

Reaction (1) has also been investigated in backward kinematics, in the region of large momentum transfer, with the aim to obtain information of transition distribution amplitudes [11]. In Ref. [12], the process

*E-mail: kuraev@theor.jinr.ru
**E-mail: bystr@theor.jinr.ru
***E-mail: bvv@jinr.ru
****E-mail: dbeyssy@ipno.in2p3.fr
†E-mail: egle.tomasi@cea.fr; permanent address: CEA, IRFU, SPhN, Saclay, 91191 Gif/Yvette Cedex, France

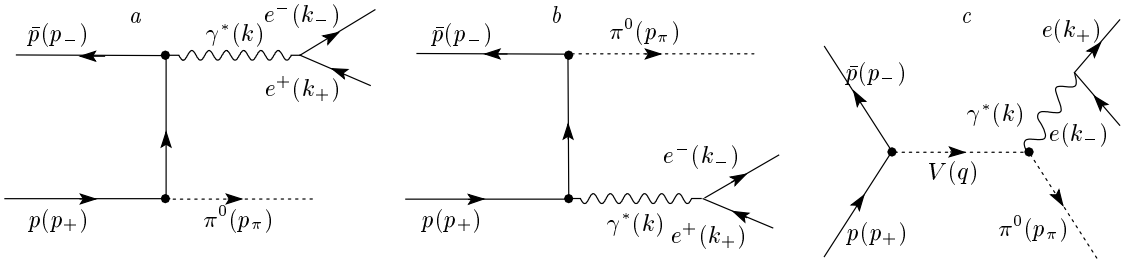

Fig. 1. Feynman diagrams (a) for $\bar{p}+p \to e^+ + e^- + \pi^0$ and (b) in the t channel ("scattering"); (c) in the s channel ("annihilation")

$p\bar{p} \to \gamma\pi^0$ was considered in the framework of the Generalized Distributions Amplitudes approach. Neither the Regge behavior of the scattering amplitude nor the resonant character of the annihilation amplitude was contained in those papers.

The reaction mechanism that allows accessing the electromagnetic structure of the proton is illustrated in Figs. 1a,b and is denoted below as the "scattering" exchange channel. In forward (backward) kinematics, the Regge character of the exchanged nucleon reveals itself. In these kinematical conditions, the exchanged nucleon is close to the mass shell. Therefore, the vertex $\gamma^* p\bar{p}$ can be described in terms of two phenomenological quantities $F_{1,2}$ that can be interpreted as proton form factors and which describe the partonic structure of the proton. This statement is valid in the kinematical region of nearly forward ($|t| \ll s$) or nearly backward ($|u| \ll s$) scattering. In the region $|t| \sim |u| \sim s \gg M_p^2$, these amplitudes are (unknown) functions of both kinematical variables. They have the form $(M_p^2/s)^n \phi(t/s)$, where the exponent n is determined by quark-counting rules, and are not related to the Dirac and Pauli form factors of the proton. A similar behavior is expected for the vertex of pion interaction with nucleons.

In collinear kinematics (nearly forward scattering and nearly backward scattering), the amplitude of the scattering channel dominates because the contribution of the annihilation channel is suppressed by the phase volume factor $|t|/s$ or $|u|/s$. At emission angles near 90° (with the center-of-mass reference frame implied), the cross section is dominated by the amplitude of the "annihilation" vector meson exchange mechanism (see Fig. 1c). Intermediate states such as nucleoniums ($p\bar{p}$ bound states) and vector and scalar mesons (including radially excited meson states) can contribute in principle. In Ref. [13], the creation of narrow resonances was discussed. We focus our interest on the energy region outside the resonance production. Heavy vector meson intermediate states such as $\omega(1450)$ and $\omega(1650)$ mesons play an important role in the limited kinematical range, where the total energy is close to their mass, due to the Breit–Wigner character of the relevant amplitudes of these states. Outside this region, they are suppressed by form factors because they are more extended objects.

In this paper, we focus on processes (1) and (2) in the kinematical region where the s channel is expected to dominate (large-angle emission of the pion and moderate values of the total energy squared, s). The characterization of this mechanism (see Fig. 1c) is important not only for disentangling the information on proton form factors (which are accessible through the "scattering" mechanism; see Figs. 1a,b) but also for gaining information on the properties of the vector mesons. Here, the parton (quark) structure of the proton turns out to be essential. We limit our considerations to the ω-exchange in the intermediate state. It is known from the literature [14, 15] that the largest anomalous vertex is $\rho\omega\pi$, because it has the largest quark coupling.

The interaction of the vector ω-meson with the nucleus in the vertex ωpp, which contains information on the strong proton and meson couplings, can be described in terms of proton vector form factors, in the time-like region of momentum transfer squared. They have a complex nature, in principle. The vertex $\omega \to \pi\gamma^*$ can be described either by a phenomenological parameterization or through a quark triangle vertex. Recently, large interest has been raised in this field by the new data from the BaBar Collaboration on the pion form factor at large momentum transfer [16].

The calculation is compared with the unpolarized cross section and with the angular distribution for $\bar{p}+p \to \gamma+\pi^0$ annihilation, which was measured in the region 2.911 GeV $\le \sqrt{s} \le$ 3.686 GeV by the Fermilab E760 Collaboration [17].

The plan of this paper is as follows. In Sec. 2, we calculate the $\bar{p}+p \to \gamma+\pi^0$ process for the annihila-

tion channel: the kinematical variables are defined, and the phase space and the matrix element of the reaction are calculated. In Sec. 3 the case of a virtual photon is considered and the double differential cross section is calculated. In Sec. 4, a realistic parameterization for the vertices and the coupling constants is presented. In Sec. 5, we compare the calculation with the data in the case of real photon emission at about 90°, and make predictions for the double differential cross section for the reaction $\bar{p}+p\to\gamma^*+\pi^0$. In Sec. 6, the applicability domain of the present model and its interference with the scattering channel exchange mechanism are discussed.

2. FORMALISM FOR $\bar{p}+p\to\gamma+\pi^0$

We first consider the process of proton–antiproton annihilation into a real photon of momentum k (with $k^2=0$) and a neutral pion:

$$\bar{p}(p_-)+p(p_+)\to\gamma(k)+\pi^0(p_\pi). \tag{3}$$

Both annihilation and scattering exchange channels play a role, as is discussed below. We first address the kinematic issue that is common to both mechanisms.

2.1. Kinematics

The calculation is performed in the center-of-mass system (c.m.s.) (Fig. 2). We fix the c.m.s. parameterization of the momenta (of the form $p=(p_0,\mathbf{p})$ where $\mathbf{p}$ is a 3-vector) as

$$p_\pm=(E,\pm\mathbf{p})=\left(\frac{\sqrt{s}}{2},\pm\mathbf{p}\right),$$

$$p_\pm^2=M_p^2,\quad k=(k_0,\mathbf{k}),$$

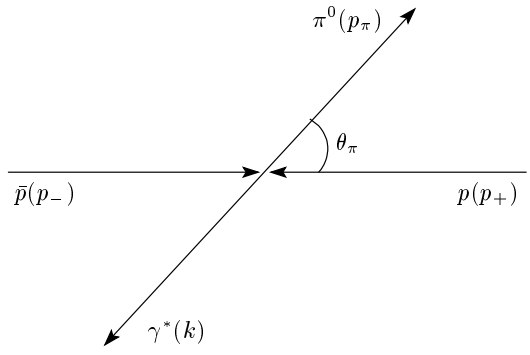

Fig. 2. Schematic view of the reaction $\bar{p}+p\to\gamma^*+\pi^0$ in the center-of-mass system

$$q=p_++p_-=(2E,0),\quad p_\pi=(E_\pi,-\mathbf{k}),$$
$$E=\frac{\sqrt{s}}{2},\quad \beta=\frac{|\mathbf{p}|}{E}=\sqrt{1-4\frac{M_p^2}{s}},$$

where E (β) is the energy (velocity) of the initial proton of mass M_p, k_0 is the energy of the emitted photon, and E_π is the pion energy. We then can calculate the necessary scalar products:

$$\begin{gathered}2(p_\pm q)=4E^2=s,\quad 2(qk)=s-M_\pi^2,\\ 2(p_\pm k)=\frac{s-M_\pi^2}{2}(1\pm\beta c_\pi),\end{gathered} \tag{4}$$

where $c_\pi=\cos(-\mathbf{k},\mathbf{p})$ is the cosine of the angle between the momenta of the initial proton and the produced pion.

For convenience, we introduce the invariant variables

$$s=(p_++p_-)^2=(k+p_\pi)^2=q^2,$$
$$u=(p_+-p_\pi)^2=(p_--k)^2,$$
$$t=(p_--p_\pi)^2=(p_+-k)^2,\quad s+t+u=2M_p^2+M_\pi^2,$$

then the relevant scalar products are

$$2(p_+p_-)=s-2M_p^2,\quad 2(p_-p_\pi)=-t+M_p^2+M_\pi^2,$$
$$2(p_+p_\pi)=-u+M_p^2+M_\pi^2,\quad 2(kp_\pi)=s-M_\pi^2,$$
$$2(p_+k)=-t+M_p^2,\quad 2(p_-k)=-u+M_p^2.$$

The phase volume of this reaction has the standard form

$$d\Phi_2=(2\pi)^4\frac{d\mathbf{k}}{(2\pi)^3 2k_0}\frac{d\mathbf{p}_\pi}{(2\pi)^3 2E_\pi}\delta^4(p_++p_--k-p_\pi)=$$
$$=\frac{s-M_\pi^2}{2^5\pi^2 s}\,d\Omega_\pi=\frac{s-M_\pi^2}{2^5\pi^2 s}\,d\Omega_\gamma, \tag{5}$$

where Ω_π and Ω_γ are the pion and photon phase volumes and the mass-shell δ-function for the final particles restricts the energies and the moduli of the momenta to

$$\begin{gathered}E_\pi=\frac{s+M_\pi^2}{2\sqrt{s}},\quad \omega=|\mathbf{k}|=|\mathbf{p}_\pi|=\frac{s-M_\pi^2}{2\sqrt{s}},\\ \beta_\pi=\frac{|\mathbf{p}_\pi|}{E_\pi}=\frac{s-M_\pi^2}{s+M_\pi^2},\end{gathered} \tag{6}$$

and β_π is the pion velocity. The cross section can be calculated using the expression

$$d\sigma=\frac{1}{4\cdot 4I}\int\sum_{spins}|\mathcal{M}|^2 d\Phi_2, \tag{7}$$

where $\mathcal{M}$ is the reaction matrix element and

$$I=\frac{1}{2}\sqrt{s(s-4M_p^2)}=\frac{s\beta}{2}$$

is the invariant flux.

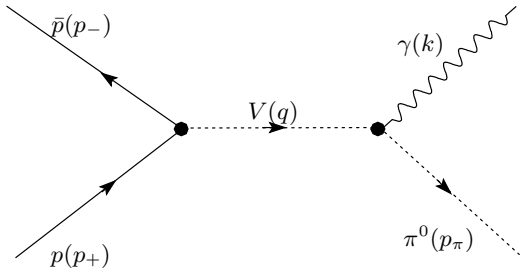

Fig. 3. Feynman diagram for the annihilation reaction $\bar{p}+p \to \gamma + \pi^0$ through a vector meson exchange

2.2. $\bar{p}+p \to \gamma + \pi^0$ annihilation through an ω-meson exchange

We consider the annihilation channel through a vector meson exchange for the reaction

$$\bar{p}(p_-) + p(p_+) \to V(q) \to \gamma(k) + \pi^0(p_\pi), \qquad (8)$$

as is illustrated in Fig. 3.

The matrix element for the exchange of an intermediate vector meson V can be written as

$$\mathcal{M}^\gamma = -\frac{G_{V\pi\gamma}(q^2,0)G_{Vpp}\epsilon_{\mu\nu\rho\sigma}e^\nu q^\rho k^\sigma}{M_V[s-M_V^2+iM_V\Gamma_V(q^2)]} \times \\ \times \left(g^{\mu\alpha} - \frac{q^\mu q^\alpha}{M_V^2}\right)\mathcal{J}_\alpha^{(V)}(s), \qquad (9)$$

where $\epsilon_{\mu\nu\rho\sigma}$ is the Levi-Civita antisymmetric tensor, $V=\rho,\ \omega,\ \ldots$, M_V and $\Gamma_V(q^2)$ are the mass and the total width of the intermediate vector meson V with momentum q ($q^2=s$), and e^μ is the polarization vector of the emitted real photon with $(ek)=0$. In principle, the total width of the intermediate vector meson depends on q^2. This dependence, which is a function of the produced particle momentum, is especially important in the case of wide resonances. It is introduced to suppress unphysical contributions outside the resonance region [18]. In the present case, because we are far from the resonance mass and consider the ω meson with a small width, we neglect the q^2 dependence of the width (i. e., $s \gg M_\omega^2, M_\omega\Gamma_\omega$).

The quantity $G_{V\pi\gamma}(q^2,k^2)$ describes the $V(q) \to \pi(p_\pi)\gamma(k)$ vertex and is given in Sec. 4. The current $\mathcal{J}_\alpha^{(V)}(q^2)$ related to the $p\bar{p}V$ vertex has the form

$$\mathcal{J}_\alpha^{(V)}(q^2) = \bar{v}(p_-)\Gamma_\alpha^{(V)}(q^2)u(p_+), \qquad (10)$$

where $\bar{v}(p_-)$ and $u(p_+)$ are spinors describing the antiproton and proton wave functions, and the vertex $\Gamma_\alpha^{(V)}$ is parameterized through two (strong) form factors $F_{1,2}^{(V)}$ as

$$\Gamma_\alpha^{(V)} = F_1^{(V)}(q^2)\gamma_\alpha + \frac{i}{2M_p}F_2^{(V)}(q^2)\sigma_{\alpha\beta}q^\beta, \qquad (11)$$

where $\sigma^{\mu\nu} = (i/2)(\gamma^\mu\gamma^\nu - \gamma^\nu\gamma^\mu)$, and the explicit expression for $F_{1,2}^{(V)}$ is given in Sec. 4.

The region of our interest is far outside the region of narrow resonances defined as $|\sqrt{s}-M_R| \sim \Gamma_R \ll \sqrt{s}$, where M_R (Γ_R) is the mass (width) of the resonance. In the region close to the resonance production, the effects of formation of bound states are very important and can drastically change the value of the cross section [13]. This effect appears in a very narrow range and it is not necessary to take it into account in our case.

In principle, all vector mesons may contribute to the intermediate state. We give the reasons why the contribution of an intermediate ω meson is dominant for this process, with respect to the ρ-exchange. The value of the Vpp coupling is $g_{\omega pp}^2/4\pi = 20 \gg g_{\rho pp}^2/4\pi = 0.55$. For the $V\pi\gamma$ vertex, the coupling of the vector meson to the quark is relevant. The coupling constants of the ω and ρ mesons with the valence quarks in the proton or pion are quite different. The ω meson, being an isotopic singlet, constructively interacts with the quarks, unlike the ρ meson, which is an isovector and its interaction with quarks is destructive. This is the reason why $g_{\omega qq} \sim 3g_{\rho qq}$. The relevant factor is large, because its square enters the amplitude. The annihilation channel contains the interaction vertex of two vector mesons with the pion. This vertex has an anomalous nature. Therefore, vector mesons must be of different species (for example, if the ρ meson is in intermediate state, then the ω meson appears in the final state). Because the ρ-meson decay width is about ten times larger than the one for the ω meson, we conclude that the main mechanism of the process under consideration is

$$p + \bar{p} \to \omega \to \pi + \rho \qquad (12)$$

with the subsequent transition of the ρ meson into a lepton pair or a real photon [19].

Concerning ρ', ω', and other radial excitations of ρ and ω mesons, an additional suppression is expected in the considered kinematical region because form factors decrease faster, describing more extended objects. We therefore consider only the contribution of the ω meson. This also simplifies the analytic calculation, because $F_2^\omega \ll F_1^\omega$ and can be neglected [20]. The vector current takes the simple form

$$\mathcal{J}_\alpha^{(\omega)}(q^2) = F_1^\omega \bar{v}(p_-)\gamma_\alpha u(p_+). \qquad (13)$$

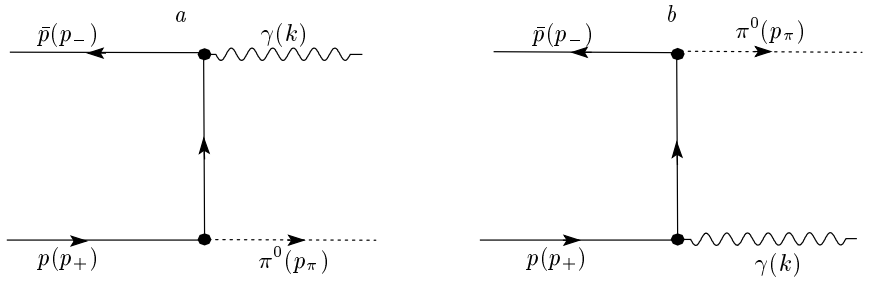

Fig. 4. Feynman diagram for the reaction $\bar{p}+p\to\gamma+\pi^0$ (a) in the t channel and (b) in the u channel

Using the relation

$$\epsilon_{\mu\alpha\rho\sigma}\epsilon_{\nu\alpha\gamma\delta}q^\rho k^\sigma q^\gamma k^\delta\sum_{spin}\mathcal{J}_p^\mu\mathcal{J}_p^{*\nu}= \\ =2s^2\mathbf{k}^2(2-\beta^2\sin^2\theta_\pi)|F_1^\omega|^2, \quad (14)$$

we obtain the differential cross section in the form

$$\left(\frac{d\sigma}{d\Omega_\gamma}\right)^{ann}=\sigma_0(q^2)(2-\beta^2\sin^2\theta_\pi),$$
$$\sigma_0(q^2)=\frac{|G_{\omega\pi\gamma}(q^2,0)|^2(q^2-M_\pi^2)^3g_{\omega pp}^2}{2^9\pi^2q^2\beta|q^2-M_\omega^2+iM_\omega\Gamma_\omega(q^2)|^2M_\omega^2}\times \quad (15)$$
$$\times|F_1^\omega|^2,$$

where the $q^2=s$ dependence is contained in σ_0, which has the dimension of a cross section. The total cross section as a function of q^2 is

$$\sigma_{ann}(q^2)=8\pi\sigma_0(q^2)\left(1-\frac{\beta^2}{3}\right). \quad (16)$$

The approximation of the ω meson in the intermediate state is well beyond the precision for the final cross section, which is evaluated to be near 10 %. This estimate takes the accuracy of the $SU(3)$ symmetry and the contributions of the neglected mesons into account.

2.3. t and u channel exchange for $\bar{p}+p\to\gamma+\pi^0$

We consider the diagrams illustrated in Fig. 4. The corresponding matrix element can be written as

$$\mathcal{M}_{sc}=eg_{\pi NN}\bar{v}(p_-)\times \\ \times\left[\gamma_5\frac{\hat{q}_1+M_p}{t-M_p^2}\Gamma_\mu+\Gamma_\mu\frac{\hat{q}_2+M_p}{u-M_p^2}\gamma_5\right]u(p_+)e^\mu, \quad (17)$$

where e is the positron charge, $g_{\pi NN}$ is the pseudoscalar coupling constant of the pion with the nucleon (the pseudovector coupling experiences momentum suppression [21]), $q_1=p_+-k$, $q_2=p_+-p_\pi$, and the proton electromagnetic vertex $\Gamma_\mu\equiv\Gamma_\mu(k^2=0)$ is parameterized in terms of the form factors $F_{1,2}$:

$$\Gamma_\mu(k^2)=F_1(k^2)\gamma_\mu+\frac{i}{2M_p}F_2(k^2)\sigma_{\mu\nu}k^\nu, \quad (18)$$

which, in the real photon limit, coincide with the static values $F_1=1$, $F_2=1.798$. The differential cross section is

$$d\sigma_{sc}=\frac{1}{8s}\sum|\mathcal{M}_{sc}|^2d\Gamma_2, \quad (19)$$

where the phase space can be written as

$$d\Gamma_2=(2\pi)^{-2}\frac{d^3k}{2k_0}\frac{d^4q}{\sqrt{s}}\delta(q^2-m_\pi^2)= \\ =\frac{1}{4\pi}k_0\,dk_0\,d\cos\theta\,\delta[(p_++p_--k)^2-M_p^2]= \\ =\frac{s-m_\pi^2}{16\pi s}d\cos\theta. \quad (20)$$

We use the relation $(p_++p_--k)^2-M^2=s-2\sqrt{s}k_0-m_\pi^2$.

The differential cross section for the t and u channels and their interference are given by

$$d\sigma=\frac{1}{2s}\,\frac{s-m_\pi^2}{16\pi s}\sum|\mathcal{M}_{sc}|^2d\cos\theta, \quad (21)$$

where

$$\sum|\mathcal{M}_{sc}|^2=e^2g_{\pi NN}^2\left(-\frac{s}{t-M_p^2}F_tR_t-\right. \\ \left.-\frac{s}{u-M_p^2}F_uR_u+\frac{s}{2M_p^2}F_2^2(s)\right), \quad (22)$$
$$F_t=F_1^2(t)+2F_1(t)F_2(t)+\frac{1}{2}F_2^2(t),$$
$$F_u=F_1^2(u)+2F_1(u)F_2(u)+\frac{1}{2}F_2^2(u).$$

The effects of strong interaction in the initial-state interaction due to an exchange by vector and (pseudo) scalar mesons between the proton and the antiproton

are quite essential in the scattering channel. They effectively lead to the Regge form of the amplitude of the scattering channel. Hence, the t and u diagrams are suppressed by the general Regge factors R_t and R_u of the form

$$R_t = R(t) = \left(\frac{s}{s_0}\right)^{2[\alpha_p(t)-1]}, \qquad \alpha_p(t) = \frac{1}{2} + r\frac{\alpha_s}{\pi}\,\frac{t-M_p^2}{M_p^2}, \tag{23}$$

$$R_u = R(u) = \left(\frac{s}{s_0}\right)^{2[\alpha_p(u)-1]}, \qquad \alpha_p(u) = \frac{1}{2} + r\frac{\alpha_s}{\pi}\,\frac{u-M_p^2}{M_p^2}, \tag{24}$$

where r and s_0 can be regarded as fitting parameters [22]. In the numerical applications below, we take $s_0 \approx 1$ GeV^2 and $r\alpha_s/\pi \approx 0.7$.

In principle, this Regge form of the amplitude incorporates an infinite number of resonances ($\Delta(1232)$ and others). The excited resonances such as $N^*(1440)$ belong to daughter Regge trajectories, which are power suppressed compared to the leading one. This is also included in the estimate of the claimed 10 % error.

3. FORMALISM FOR THE REACTION $\bar{p}+p\to e^+ + e^- + \pi^0$

We consider the annihilation channel of the reaction

$$\bar{p}(p_-) + p(p_+) \to \gamma^*(k) + \pi^0(p_\pi) \to \to e^+(k_+) + e^-(k_-) + \pi^0(p_\pi), \tag{25}$$

where the four momenta of the particles are indicated in parentheses.

We focus here on the mechanism of annihilation through an ω meson exchange. The general expression for the matrix element corresponding to the diagram in Fig. 1*c* for the exchange of a vector meson V is

$$\mathcal{M}^{\pm} = 4\pi\alpha\frac{G_{V\pi\gamma^*}(q^2,k^2)g_{Vpp}}{e} \times \frac{\epsilon_{\mu\nu\rho\sigma}q^\rho k^\sigma}{k^2 M_V(q^2-M_V^2+iM_V\Gamma_V)}\mathcal{J}_p^\mu\mathcal{J}_e^\nu, \tag{26}$$

where $e=\sqrt{4\pi\alpha}$ is the elementary electric charge ($\alpha\approx 1/137$). The lepton electromagnetic current has the standard form

$$\mathcal{J}_e^\nu = \bar{u}(k_-)\gamma^\nu v(k_+), \tag{27}$$

and the electromagnetic current related to the $p\bar{p}V$ vertex is

$$\mathcal{J}_p^\mu = \bar{v}(p_-)\Gamma_\omega^\mu u(p_+), \quad \Gamma_\omega^\mu = F_1^\omega(q^2)\gamma^\mu. \tag{28}$$

The currents are gauge invariant:

$$k_\nu\mathcal{J}_e^\nu = q_\mu\mathcal{J}_p^\mu = 0.$$

Again, only the ω exchange is considered and F_2 is neglected.

The cross section of process (25) can be written in the standard form

$$d\sigma = \frac{1}{4I}\int\sum_{spin}|\mathcal{M}|^2 d\Phi_3, \tag{29}$$

where $d\Phi_3$ is the phase volume of the process,

$$d\Phi_3 = (2\pi)^4\delta^4(p_+ + p_- - k_+ - k_- - p_\pi)\times \times\frac{d^3k_+}{(2\pi)^3 2E_+}\,\frac{d^3k_-}{(2\pi)^3 2E_-}\,\frac{d^3p_\pi}{(2\pi)^3 2E_\pi} = = \frac{1}{(2\pi)^4}\beta_\pi E_\pi\,dE_\pi\,dc_\pi\frac{1}{2}d\Phi_e, \qquad d\Phi_e = \frac{d^3k_+}{2E_+}\,\frac{d^3k_-}{2E_-}\delta^4(k-k_+-k_-), \tag{30}$$

where E_+, E_- and E_π are the electron, positron, and pion energies in the final state.

Because our aim is to calculate the angular distribution and energy spectrum of the final pion, we insert the unit integration

$$\int d^4k\;\delta^4(k-k_+-k_-) = 1. \tag{31}$$

Performing the integration over the final lepton momenta,

$$\int d\Phi_e\sum_{spin}\mathcal{J}_e^\mu\mathcal{J}_e^{*\nu} = = -\frac{2\pi}{3}k^2\left(g^{\mu\nu}-\frac{k^\mu k^\nu}{k^2}\right)\phi(k^2), \tag{32}$$

where

$$\phi(k^2) = \left(1+\frac{2m_e^2}{k^2}\right)\sqrt{1-\frac{4m_e^2}{k^2}}, \tag{33}$$

we obtain the following expression for the double differential cross section:

$$d^2\sigma^{\pm} = \sigma_0^{\pm}dW, \qquad \sigma_0^{\pm}(q^2) = \frac{\alpha(q^2)^2|G_{\omega\pi\gamma^*}(q^2,k^2)|^2|F_1^\omega(q^2)|^2 g_{\omega pp}^2}{\beta M_\omega^2\left[(q^2-M_\omega^2)^2+M_\omega^2\Gamma_\omega^2\right]}, \qquad dW = \frac{\beta_\pi^3 E_\pi^3(2-\beta^2\sin^2\theta_\pi)}{48s\pi^2k^2}\phi(k^2)dE_\pi dc_\pi, \qquad k^2 = s+M_\pi^2-2E_\pi\sqrt{s} > 4m_e^2, \tag{34}$$

where we set $k^2 = 0$ in the vertex $\omega\pi\gamma^*$ because we consider the case of small virtuality. The energy of the final pion distribution can be obtained by integrating over the angle:

$$\frac{d\sigma^{\pm}}{dE_\pi} = \int\limits_{-1}^{1} dc_\pi \frac{d^2\sigma^{\pm}}{dE_\pi dc_\pi} = \\ = \sigma_0^{\pm}(q^2)\frac{\beta_\pi^3 E_\pi^3}{12\,q^2\pi^2\,k^2}\phi(k^2)\left(1-\frac{\beta^2}{3}\right), \\ \beta_\pi E_\pi = \sqrt{E_\pi^2 - M_\pi^2}. \tag{35}$$

4. MODELS OF FORM FACTORS AND VERTICES

In principle, we should include initial-state interaction that strongly modifies the cross section at near-threshold energies. It is evaluated introducing a multiplicative factor C, the Coulomb factor, which takes multiphoton exchanges into account:

$$C = \frac{x}{e^x - 1}, \quad x = \frac{\alpha\pi}{v}, \tag{36}$$

where v is the incident relative velocity in c units. In the high-energy range considered here, this factor is close to unity. In our case, this factor increases the cross section, because the interaction occurs between opposite charges. For example, $C = 1.6$ at $\sqrt{s} = 2$ GeV and $v = 0.34c$. As regards meson exchanges, we recall that in $\bar{p}p$ annihilation, one pion exchange is suppressed by the factor M_p^2/s, which becomes more and more important at high energies, the ω meson is included in the ωNN form factor, and heavier vector meson are suppressed for the reasons given above.

Following [23], the form factor $F_{1,2}^{\omega}(q^2)$ can be parameterized as

$$F_1^{\omega}(q^2) = \frac{\Lambda_\omega^4}{\Lambda_\omega^4 + (q^2 - M_\omega^2)^2} \tag{37}$$

with the normalization $F_1^{\omega}(M_\omega^2) = 1$. Here $\Lambda_\omega = 1.25$ GeV is an empirical cut-off. We set $M_\omega = 782.65 \pm 0.19$ MeV.

This parameterization is constructed for the space-like region of momentum transfer. In the time-like region, we should consider an analytic extension of this formula, introducing an imaginary part in particular. This procedure has been suggested for electromagnetic form factors of the nucleon in [24], for the ρ meson in [25], and for the a_1 meson in [26]. Such parameterizations are very reliable when data exist to constrain the parameters. This is not the present case, and such a procedure would add more uncertainties.

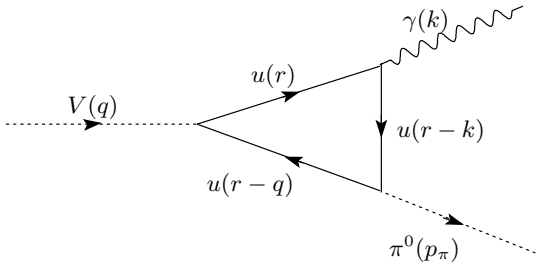

Fig. 5. Triangle diagram for $V \to \pi\gamma$

The quantity $G_{\omega\pi\gamma^*}$ is related to the matrix element of the transition $\omega(q) \to \pi(p)\gamma(k)$ (Fig. 5) and it is in principle momentum dependent:

$$\mathcal{M}(\omega \to \pi\gamma) = \frac{G_{\omega\pi\gamma^*}}{M_\omega}(q^2, k^2)\epsilon_{\mu\nu\alpha\beta}q^\alpha k^\beta \epsilon_\omega^\mu \epsilon_\gamma^\nu, \tag{38}$$

where we introduce the polarization vectors of the photon ϵ_γ^μ and the vector meson ϵ_ω^ν. It can be calculated as [27]

$$|G_{\omega\pi\gamma}(q^2, k^2)|^2 = 9\frac{\alpha}{\pi^3}\frac{g_{\omega uu}^2 M_\omega^2}{F_\pi^2}|I(q^2, k^2)|^2, \tag{39}$$

where we use the Goldberger–Treiman relation $g_{\pi uu}/m_u = 1/F_\pi$, and $F_\pi = 93$ MeV [19] is the pion decay constant. The constants $g_{\omega uu}$ and $g_{\pi uu}$ correspond to the coupling of ω and π mesons to the light u quarks in the loop. We take the values $g_{\omega uu} = 5.94$ and $g_{\pi uu} = 2.9$ [28]. The internal quark loop integral $I(q^2, k^2)$ is derived in Appendix A. Due to the requirement of the absence of a real quark in the intermediate state, the quantity $I(q^2, k^2)$ must be real:

$$I(q^2, k^2) = \frac{m_u^2}{2(k^2 - s)}\left(\ln^2\frac{q^2}{m_u^2} - \ln^2\frac{k^2}{m_u^2}\right), \\ k^2 \gg m_u^2, \quad q^2 \gg m_u^2, \tag{40}$$

where m_u is the constituent quark mass. We verified that our results for real and virtual photons agree in the limit $k^2 \to m_u^2$:

$$I(s, k^2 \to m_u^2) \approx -\frac{m_u^2}{2s}\ln^2\frac{s}{m_u^2}. \tag{41}$$

To check the consistency of the parameter values, we evaluate the width of the radiative decay $\omega \to \pi\gamma$:

$$\Gamma(\omega \to \pi^0\gamma) = \frac{\alpha}{192}\frac{M_\omega^3}{F_\pi^2}\frac{g_{\omega uu}^2}{\pi^4}\left(1 - \frac{M_\pi^2}{M_\omega^2}\right)^3 \approx \\ \approx 550 \text{ keV}. \tag{42}$$

Hence, the decay branching is equal to

$$\mathrm{BR}(\omega \to \pi^0\gamma) = \frac{\Gamma(\omega \to \pi^0\gamma)}{\Gamma_\omega} = 6.5\,\%, \qquad (43)$$

which is in a fair agreement with the value [19]

$$\mathrm{BR}^{exp}(\omega \to \pi^0\gamma) = (8.28 \pm 0.28)\,\%.$$

The values of the constants used in the calculation are $\Gamma_\omega = 8.49 \pm 0.08$ MeV, $\mathrm{BR}(\omega \to \pi\gamma) = (8.28 \pm 0.28) \cdot 10^{-2}$, $\Gamma_{\omega\to\pi\gamma} = 0.70297$ MeV, and $g^2_{\omega NN}/4\pi = 20$.

Alternatively, one can choose a phenomenological parameterization for the vertex $\omega \to \pi\gamma^*$, based on the monopole dependences on q^2 and k^2:

$$G_{\omega\pi\gamma^*}(q^2,k^2) = \frac{G_{\omega\pi\gamma}(0,0)}{(1+q^2/M_\omega^2)(1+k^2/M_\omega^2)}, \qquad (44)$$

where the constant $G_{\omega\pi\gamma}(0,0)$ is derived from the radiative decay $\omega \to \pi\gamma$ [29]:

$$\Gamma(\omega \to \pi\gamma) = \frac{M_\omega \alpha}{24}|G_{\omega\pi\gamma}(0,0)|^2 \left(1 - \frac{M_\pi^2}{M_V^2}\right)^3. \qquad (45)$$

5. RESULTS

No experimental data exist on the reaction $\bar{p}+p \to e^+ + e^- + \pi^0$, but the reaction $\bar{p}+p \to \gamma+\pi^0$ was measured in the region 2.911 GeV $\le \sqrt{s} \le$ 3.686 GeV by the Fermilab E760 Collaboration [17] and data exist on the cross section and the angular distribution. It is in principle possible to adapt the present model to γ production and compare the calculation to the data in the angular region around 90°, where the present mechanism is expected to be dominant (Fig. 6).

A good agreement with the existing data can be obtained for parameterization (39) of the coupling constant $g_{V\pi\gamma}$, by including the additional coupling factor

$$F_{1q}^{\omega}(q^2) = \left[\frac{\Lambda_\omega^4}{\Lambda_\omega^4 + (q^2 - M_\omega^2)^2}\right]^{1/3}, \qquad (46)$$

due to the interaction of the vector meson with the constituent quarks in the $Vu\bar{u}$ vertex. A good agreement with the data is also obtained using phenomenological parameterization (44) and $\Lambda_\omega = 1.25$ GeV. This is shown in Fig. 7, where the results on the cross section integrated in the range $|\cos\theta_\pi| < 0.2$ are reported and compared with the present calculation in s channel.

In Fig. 6, the angular distributions are shown for four values of the total c.m.s. energy together with the results of the calculation. A good agreement for the

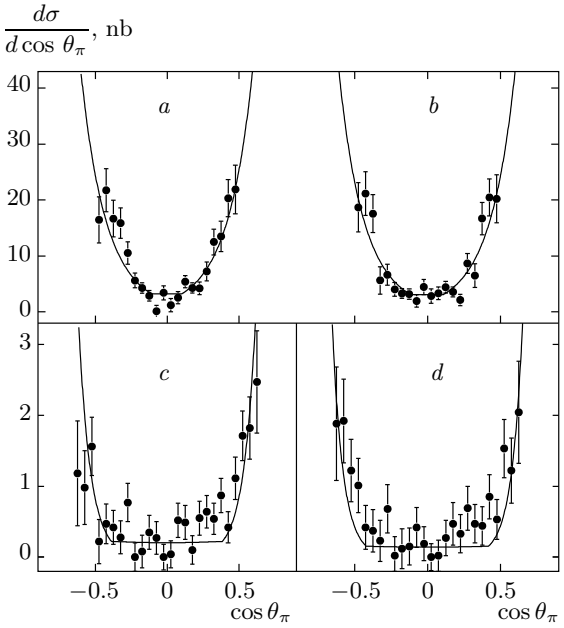

Fig. 6. Angular distributions for different values of the c.m.s. energy: (*a*) $\sqrt{s} = 2.975$ GeV; (*b*) $\sqrt{s} = 2.985$ GeV; (*c*) $\sqrt{s} = 3.591$ GeV; (*d*) $\sqrt{s} = 3.686$ GeV. The data are from [17], the line is the result of our model

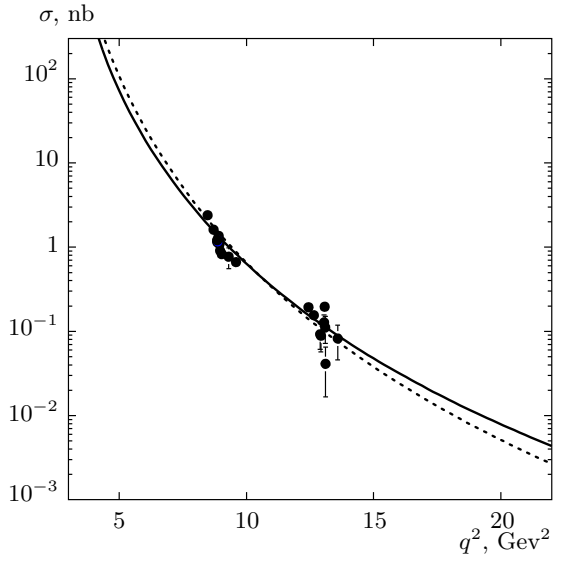

Fig. 7. q^2 dependence of the cross section. The data and the calculations are integrated for $|\cos\theta_\pi| < 0.2$ for two choices of the $G_{\omega\pi\gamma}$ coupling: from parameterizations (39) (dashed line) and from the monopole dependence (solid line); experimental data from [17]

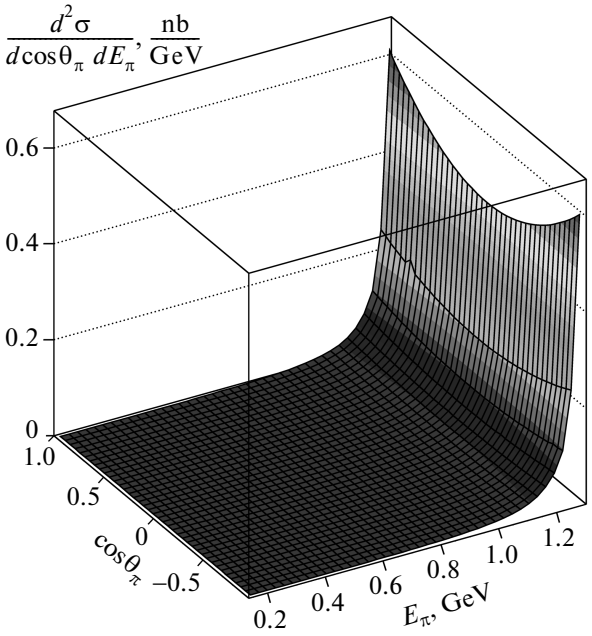

Fig. 8. Bidimensional plot of the double differential cross section for the process $\bar{p} + p \to \gamma^* + \pi^0$ as a function of E_π and $\cos\theta_\pi$ at $q^2 = 7$ GeV^2

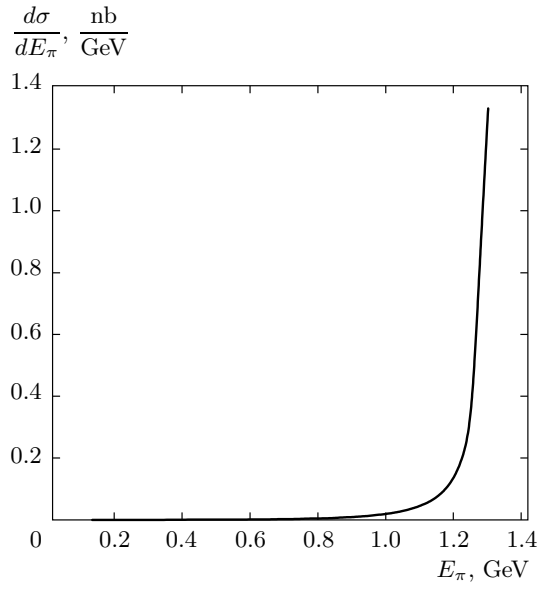

Fig. 9. Differential cross section for the process $\bar{p}+p \to \gamma^* + \pi^0$ as a function of E_π at $q^2 = 7$ GeV^2

s-channel calculation, Eq. (15), is obtained in the angular region around $\cos\theta_\pi \approx 0$, because, as expected, this mechanism is applicable at these angles.

To reproduce the data in the full range where they are available, we have to also consider t and u exchanges. Here, we focus on the s-channel properties and apply a simplified procedure with the s, t, and u channels considered in separated kinematical regions, hence neglecting their interference.

It follows from the data that the angular distribution flattens in a range around $\cos\theta \approx 0$, which depends on s. In this central region, we use the s-channel result, Eq. (15). In the forward and backward regions, we use Eq. (21), where the u and t contributions contain suppression due to Regge factors $R_{u,t}$. The results are shown in Fig. 6.

For the s-channel annihilation, which is the subject of this paper, the differential and total cross sections have been numerically calculated for the reaction $\bar{p} + p \to e^+ + e^- + \pi^0$ and the results are illustrated for $q^2 = 7\,\text{GeV}^2$ and for parameterization (39) of the $\omega\pi\gamma^*$ vertex.

The bidimensional plot of the cross section as a function of the c.m.s. angle and energy of the pion is shown in Fig. 8. The angular and energy dependences are fixed by the model. The absolute value of the cross section strongly depends on the cutoff parameter taken for the description of the ωNN vertex, which was taken here as for the real photon data.

For a virtual photon, the $G_{\omega\pi\gamma}$ coupling depends on q^2 and k^2. The phenomenological parameterization can be modified by adding a monopole dependence on k^2. For parameterization (39), the triangle integral has a more complicated form in general [30]. Neglecting the pion mass, we can use the symmetry properties of the triangle loop (see the Appendix).

The bidimensional cross section as a function of the pion variables, at the fixed total energy $s = 7$ GeV^2, is shown in Fig. 8 and the projection on the pion energy is plotted in Fig. 9 for parameterization (39) of the $G_{V\pi\gamma}$ vertex. It can be seen that the cross section has a smooth angular dependence and it is the larger, the higher the pion energy.

6. DISCUSSION AND CONCLUSIONS

We have presented hadronic model for the annihilation channel in the processes $p + \bar{p} \to \pi^0 + \gamma(\gamma^*)$. This reactions is described by two classes of diagrams. We focused here on the annihilation-type diagrams. The scattering-type diagrams with a nucleon in the intermediate state were considered earlier, in Ref. [5] and the references therein.

We considered the ω-meson intermediate state as the main contribution because it contains the same u and d quarks as the final π^0, excluding the ρ meson

due to the small ρNN coupling as well as higher resonances. We applied our calculation in the energy region outside the resonance production. We compared our calculation to the existing data on $p\bar{p} \to \pi^0\gamma$ and found a good description also taking the t and u channels into account, in forward and backward angular regions. The formulas obtained in this paper describe the annihilation channel through the ω meson (which makes an almost isotropic contribution in the c.m.s.) as well as the near-forward or near-backwards kinematics (Reggeized nucleon in t and u channels). We reproduce the experimental evidence that the range of the central angular region where s channel dominates increases as the energy increases.

As was shown in Ref. [5], the contribution of the t channel can be parameterized in terms of two unknown functions $F_{1,2}(t,u)$ that depend on both variables t and u ($s+t+u=2M^2$) and rapidly decrease in the region $s \sim |t| \sim |u|$ as $F_{1,2}(t,u) \sim (M^2/s)^n \ll 1$, where $n > 1$. We note that in the limits $|t| \ll s$ or $|u| \ll s$, these quantities do coincide with the electromagnetic form factors of the proton. In these kinematical regions, the Regge factors have to be included into the differential cross section. These factors suppress the cross section rather strongly.

The initial-state interaction through a meson exchange is effectively taken into account in our calculation as follows.

1. In the annihilation channel, it is in principle included in the form factors that describe the vertex $\bar{p}p\omega$, which is in principle complex. We note that in the model that we use and which was described in [23], this coupling is real. In general, it is possible to use parameterizations built for the space-like region and make an analytic continuation to the time-like region. But any extension of the parameterization requires extra parameters that cannot be presently constrained and induces unnecessary complications in the model.

2. In the scattering channel, the initial-state interaction effects are included in the Regge factor of the amplitudes.

We note that in the case of γ^* production, with the subsequent conversion to an electron–positron pair, in the annihilation channel, we can take an intermediate ρ-meson production from ω into account by the replacement

$$\frac{e^2}{k^2} \to \frac{G_{\rho e^+e^-}G_{\rho uu}}{k^2 - M_\rho^2 + iM_\rho\Gamma\rho}, \tag{47}$$

where $G_{\rho uu} = G_{\rho pp}$ and $G_{\rho e^+e^-}$ is determined from the width of the decay $\rho \to e^+ + e^-$:

$$G^2_{\rho e^+e^-} = \frac{12\pi\Gamma_{\rho\to e^+e^-}}{M_\rho} \tag{48}$$

with $\Gamma_{\rho e^+e^-} = 7 \cdot 10^{-3}$ MeV [19].

We estimate the accuracy of our calculation to be about 10 %, which is evaluated from the precision of the $SU(3)$ symmetry and the contributions of other vector mesons that we do not consider here.

The present approach can be generalized to all pseudoscalar mesons, π, η, η', and so on.

The authors are grateful to G. I. Gakh, J. Van de Wiele, and S. Ong for the interesting discussions and remarks. This work was done in the framework of the JINR–IN2P3 collaboration agreement and GDR n. 3034 "Physique du Nucléon" (France) and partly supported by the grants RFBR 10-02-01295 and Bielorussia-JINR 2010. One of us (A. D.) acknowledges the Libanese CNRS for financial support. Besides, one of us (Yu. M. B.) acknowledges a 2011 grant for JINR Young Scientists for financial support.

APPENDIX

Loop integral

In (39), the vertex $V(q) \to \pi(p_\pi)\gamma(k)$ was expressed in terms of the quark loop integral

$$I(q^2,k^2) = -\int \frac{d^4p_q}{i\pi^2} m_u^2 \times$$

$$\times \left\{(p_q^2 - m_u^2 + i0)\left[(p_q-q)^2 - m_u^2 + i0\right] \times\right.$$

$$\left. \times \left[(p_q-k)^2 - m_u^2 + i0\right]\right\}^{-1} = \int\limits_0^1 dx \times$$

$$\times \int\limits_0^{1-x} dy \left(1 - \frac{q^2}{m_u^2}xy - \frac{k^2}{m_u^2}xz - \frac{M_\pi^2}{m_u^2}yz - i0\right)^{-1}, \tag{A.1}$$

where m_u is the mass of the u quark that circulates in the loop. The value of this integral in the case of a real photon (i. e., $k^2 = 0$) is well known (see, e. g., Ref. [31]):

$$I(q^2,0) = I_2\left(\frac{q^2}{m_u^2}, \frac{M_\pi^2}{m_u^2}\right), \tag{A.2}$$

where $I_2(a,b)$ was defined in [31]:

$$I_2(a,b) = \frac{2}{a-b}\left[f\left(\frac{1}{b}\right) - f\left(\frac{1}{a}\right)\right], \tag{A.3}$$

$$f(x) = \begin{cases} -\left[\arcsin\left(\dfrac{1}{2\sqrt{x}}\right)\right]^2, & x > \dfrac{1}{4}, \\ \dfrac{1}{4}\left[\ln\left(\dfrac{\eta_+}{\eta_-}\right) - i\pi\right]^2, & x < \dfrac{1}{4}, \end{cases} \tag{A.4}$$

and $\eta_\pm = \left(1 \pm \sqrt{1-4x}\right)/2$. Applying this formula in the triangle Feynman diagram to the quark loop in the intermediate state, we must drop the imaginary term $i\pi$ (see Fig. 5). In accordance with the confinement property, real quarks on the mass shell are not allowed.

In the process involving a virtual photon (i. e., $k > 0$), the above integral has a more complicated form. But we can find a simple expression neglecting the pion mass. Indeed, expression (A.1) is symmetric with respect to q^2, k^2, and M_π^2, and therefore we can use Eq. (A.4) with

$$I(q^2, k^2) = I_2\left(\frac{q^2}{m_u^2}, \frac{k^2}{m_u^2}\right).$$

REFERENCES

1. The PANDA, M. F. M. Lutz, B. Pire, O. Scholten, and R. Timmermans, Physics Performance Report for PANDA: Strong Interaction Studies with Antiprotons (GSI, 2009), arXiv:0903.3905.
2. Facility for Antiproton and Ion Research (FAIR), http://www.gsi.de/FAIR.
3. E. Tomasi-Gustafsson and M. P. Rekalo, arXiv: 0810.4245.
4. M. Sudol, M. Mora Espi, E. Becheva et al., Eur. Phys. J. A **44**, 373 (2010).
5. C. Adamuscin, E. A. Kuraev, E. Tomasi-Gustafsson, and F. E. Maas, Phys. Rev. C **75**, 045205 (2007).
6. M. Osipenko, arXiv:0912.5309.
7. M. P. Rekalo, Yad. Fiz. **1**, 760 (1965).
8. Collaboration High Acceptance Di-Electron Spectrometer (HADES), http://www-hades.gsi.de.
9. A. Z. Dubnickova, S. Dubnicka, and M. P. Rekalo, Z. Phys. C **70**, 473 (1996).
10. C. Adamuscin, E. Tomasi-Gustafsson, E. Santopinto, and R. Bijker, Phys. Rev. C **78**, 035201 (2008).
11. B. Pire and L. Szymanowski, Phys. Lett. B **622**, 83 (2005).
12. P. Kroll and A. Schafer, Eur. Phys. J. A **26**, 89 (2005).
13. B. Kerbikov and D. Kharzeev, Phys. Rev. D **51**, 6103 (1995).
14. E. Witten, Nucl. Phys. B **223**, 422 (1983).
15. O. Kaymakcalan, S. Rajeev, and J. Schechter, Phys. Rev. D **30**, 594 (1984).
16. The BABAR, B. Aubert et al., Phys. Rev. D **80**, 052002 (2009).
17. Fermilab E760, T. A. Armstrong et al., Phys. Rev. D **56**, 2509 (1997).
18. A. B. Arbuzov, E. A. Kuraev, and M. K. Volkov, Phys. Rev. C **C83**, 048201 (2011).
19. Particle Data Group, K. Nakamura et al., J. Phys. G **37**, 075021 (2010).
20. R. Machleidt, Phys. Rev. C **63**, 024001 (2001).
21. S. Gasiorowicz, *Elementary Particle Physics*, John Wiley and Sons, New York (1969).
22. A. B. Kaidalov, arXiv:hep-ph/0103011.
23. C. Fernandez-Ramirez, E. Moya de Guerra, and J. M. Udias, Ann. Phys. **321**, 1408 (2006).
24. E. Tomasi-Gustafsson, F. Lacroix, C. Duterte, and G. I. Gakh, Eur. Phys. J. A **24**, 419 (2005).
25. C. Adamuscin, G. I. Gakh, and E. Tomasi-Gustafsson, Phys. Rev. C **75**, 065202 (2007).
26. E. Tomasi-Gustafsson, G. I. Gakh, and C. Adamuscin, Phys. Rev. C **77**, 065214 (2008).
27. M. Volkov and V. Pervushin, *Sushchestvenno Nelinejnye Kvantovye Teorii, Dinamicheskie Simmetrii i Fizika Mezonov*, Atomizdat, Moscow (1978) [in Russian].
28. M. K. Volkov, E. A. Kuraev, and Y. M. Bystritskiy, Yad. Fiz. **72**, 1567 (2009).
29. M. P. Rekalo, J. Arvieux, and E. Tomasi-Gustafsson, Phys. Rev. C **65**, 035501 (2002).
30. L. Ametller, L. Bergstrom, A. Bramon, and E. Masso, Nucl. Phys. B **228**, 301 (1983).
31. J. F. Gunion, G. L. Kane, and J. Wudka, Nucl. Phys. B **299**, 231 (1988).